

Improved optical design for the Large Synoptic Survey Telescope (LSST)

Lynn G. Seppala, University of California, Lawrence Livermore National Laboratory

ABSTRACT

This paper presents an improved optical design for the LSST, an $f/1.25$ three-mirror telescope covering 3.0 degrees full field angle, with 6.9 m effective aperture diameter. The telescope operates at five wavelength bands spanning 386.5 nm to 1040 nm (B, V, R, I and Z). For all bands, 80% of the polychromatic diffracted energy is collected within 0.20 arc-seconds diameter. The reflective telescope uses an 8.4 m $f/1.06$ concave primary, a 3.4 m convex secondary and a 5.2 m concave tertiary in a Paul geometry. The system length is 9.2 m. A refractive corrector near the detector uses three fused silica lenses, rather than the two lenses of previous designs. Earlier designs required that one element be a vacuum barrier, but now the detector sits in an inert gas at ambient pressure, with the last lens serving as the gas barrier. Small adjustments lead to optimal correction at each band. Each filter has a different axial thickness, and the primary and tertiary mirrors are repositioned for each wavelength band. Features that simplify manufacturing include a flat detector, a far less aspheric convex secondary (10 μm from best fit sphere) and reduced aspheric departures on the lenses and tertiary mirror. Five aspheric surfaces, on all three mirrors and on two lenses, are used. The primary is nearly parabolic. The telescope is fully baffled so that no specularly reflected light from any field angle, inside or outside of the full field angle of 3.0 degrees, can reach the detector.

Keywords: astronomical telescopes, wide field telescopes, three mirror telescopes, survey telescopes, optical design, telescope design, telescope baffles

1. SPECIFICATIONS

The Large-aperture Synoptic Survey Telescope (LSST) is a proposed 8.4-meter diameter, 7-degree² field telescope. The product of collecting area and field of view will be 20 times greater than any observatory now operating or under construction. An array of CCD totaling several giga-pixels will collect data with expected exposure times of 10 to 20 seconds. This telescope will survey large portions of the sky to visual magnitudes of 24 or more, searching for Earth-threatening asteroids or probing the nature of dark energy. Good telescopes at the best sites will deliver images of 0.5 arc-sec on occasion, more frequently in the near infrared. The LSST should perform significantly better than this for each photometric spectral band to avoid further degradation of the image. The pixel sampling should be at least 0.25 arc-sec (the Nyquist sampling criterion). Using this criterion, a 1.4 giga-pixel array is needed. About 1.0 terabyte of data could be collected per viewing night.

Table 1 summarizes the parameters of recent designs. The LSST uses an 8.4 m diameter primary in a telescope with a 10.5 m focal length. The focal ratio is $f/1.25$. A detector 55 cm in diameter is necessary for a full 3 degrees field of view. The area obscuration on-axis is 25%, rising to 38% at full field. The telescopes were designed to operate at five photometric spectral bands. Spectral filters are thus required. Since the filter and any required window lead to chromatic focal shifts and aberrations, aspheric lens correctors were used to compensate these effects. With these modifications, one-third arc-second images could be achieved over all bands.

PARAMETER	VALUE	PARAMETER	VALUE
Maximum diameter	8.4 meters	Maximum length	9.0 meters
Focal length	10.5 meters	Focal ratio	$f/1.25$
Plate scale	51 μm / arc-sec	Focal surface	weakly curved aspheric
Full field of view	3.0 degrees	Detector diameter	0.55 meters
Design type	3-mirror Paul-Baker	Design modifications	two corrector lenses
Obscuration	25% on axis	Obscuration	38% full field

Table 1. First order optical specifications for previous versions of the LSST telescope.

Additional specifications and proposed operating conditions along with science goals are summarized in this conference proceedings.¹

2. PREVIOUS DESIGN HISTORY

The history of three-mirror telescopes that cover wide fields goes back to M. Paul² in 1935, as nicely summarized by Wilson³. Paul recognized that a Mersenne telescope, a pair of concave and convex paraboloids, was corrected for spherical aberration, coma and astigmatism. Knowledge of basic aberration theory led to a three-mirror design, corrected for these three aberrations, in which both the secondary and tertiary mirrors are spherical. A spherical tertiary mirror of equal but opposite curvature of the secondary mirror was added to form a real focus. The tertiary mirror was placed with its center of curvature at the vertex of the secondary mirror. The spherical aberration correction required for the tertiary mirror was achieved by **removing** the parabolic figure of the secondary. In effect, this three-mirror reflector is equivalent to a refractive Schmidt-Cassegrain telescope. There are few degrees of freedom, given that the beam is collimated between the secondary and tertiary. Once the primary mirror diameter and focal ratio are chosen, the only remaining degree of freedom is the beam reduction ratio on the secondary. Paul chose this reduction ratio to ensure that the tertiary mirror was located in front of the primary. Baker⁴ and Willstrop⁵ refined the Paul design to create telescopes with larger fields of view. The tertiary was placed well behind the primary mirror. Baker allowed the secondary mirror to have an aspheric profile and removed the restriction of matching the curvature of the tertiary. As a result, a flat field could be achieved. Telescopes of a few meters in diameter, operating around $f/2$ to $f/3$ and covering 3 or 4-degree fields, could achieve near diffraction-limited performance. Angel, Lessor and Sarlot⁶ demonstrated that a compact telescope design operating at a faster focal ratio and covering a wide field could satisfy the demanding imaging performance required by LSST. Angel et al added two corrector lenses to compensate for chromatic shifts of the spectral filter to achieve one-third arc-second images. All these designs have collimated beams between the secondary and tertiary. The field angle is set by a combination of imaging performance, baffling against stray light and the increased obscuration due to baffles off-axis.

3. CURRENT DESIGN STUDY PARAMETERS

A design study was undertaken starting about 15 months ago to determine if improvements to the existing LSST design could be achieved. The first-order design was generally maintained, since it met the scientific goals and produced a relatively compact design. However, the list of parameters explored gradually grew. The number, complexity in terms of polynomial terms and distribution of aspheric surfaces were examined. The focal ratio of the primary was allowed to vary. The restriction of a collimated beam reflected from the secondary was lifted, which led to changes in the on-axis obscuration and required baffles. All designs were required to be fully baffled such that no directly reflected light from the tertiary could reach the detector. Previous designs were baffled so that no light from within the specified field of view could reach the detector. Some light, although badly aberrated, could reach the detector from field angles exceeding the full field angle. Finally, an extra lens element was added near the detector to form a triplet lens corrector.

Several strategies helped to maintain a solution that is reasonable to fabricate and test. Aspheric surfaces were simplified in a number of ways. A minimum number of aspheric surfaces was used. In addition, high order aspheric terms were employed only when necessary. As aspheric terms are added, more rays and field points are required during optimization to ensure a valid figure of merit for the optimization procedure. If too many terms were allowed, steep aspheric gradients could result. Aspheric departures from best-fit spheres were monitored and controlled during optimization. In particular, close attention was paid to minimizing the aspheric departure on the convex secondary to ease fabrication and testing. Finally, reasonable center and edge thickness were maintained. Edge thickness of positive lenses and the center thickness of the negative lens were kept at 2 cm. The plane parallel spectral filters were required to be at least 1.25 cm thick.

Table 2 shows parameters that significantly changed during the design evolution. The focal ratio of the primary increased slightly, from $f/1.0$ to $f/1.07$. In addition, the beam became divergent at $f/12$ after reflection from the secondary mirror. The expanding beam from the secondary required several associated changes to maintain 38% obscuration at full field. The hole in the primary mirror was made larger to avoid excessive vignetting. As a result, the on-axis area obscuration for this design increased from 25% to 30% and the tertiary mirror grew in diameter by 0.3 meters. An extra lens was added to form a triplet lens corrector. The secondary asphericity has been substantially reduced to only 10 microns from the best-fit sphere. The focal surface tended to be almost flat, so that a flat focal plane could be specified without penalizing optical imaging. The five spectral filters were allowed to have different thickness.

Parameter	Earlier designs	New design
Primary focal ratio	f / 1.0	f / 1.07
Beam divergence between secondary and tertiary	collimated	f / 12 diverging
tertiary diameter	4.9 m	5.2 m
area obscuration: on-axis	25%	30%
area obscuration: full field	38%	38.6%
Number of corrector lenses	2	3
Secondary mirror: aspheric departure from best-fit sphere	>150 microns	<10 microns
Focal plane surface	curved aspheric	flat
Thickness of spectral filters	constant	varies: 12.5 mm to 21 mm
Images: 80% polychromatic diffraction	< 0.33 arc-sec	< 0.20 arc-sec

Table 2. Significant changes in the new telescope design

There are several reasons for the improvement in performance of this telescope. Increasing the focal ratio of the primary, from f/1.0 to f/1.07, reduces aberrations that must be dealt with elsewhere in the telescope. Allowing the beam to diverge at f/12 from the secondary has similar advantages. The effective focal ratio of the secondary goes from f/1.0 to f/1.09, and of the tertiary from f/1.25 to f/1.4. Table 3 shows the amount of reduction in primary wavefront aberrations for each of the mirrors, assuming that the contributions scale as a power of the effective focal ratios. One sees that third order aberrations are reduced by 20% to 36%.

Mirror	Old effective focal ratio	New effective focal ratio	Reduction in 4 th order (SA3)	Reduction in 3 rd order (CMA3)	Reduction in 2 nd order (AST3)
Primary	1.0	1.07	24%	18%	13%
Secondary	1.0	1.09	29%	23%	16%
Secondary	1.25	1.40	36%	29%	20%

Table 3. Estimates of aberration reduction based on increasing the effective focal ratios of each mirror

A triplet lens corrector has sufficient design variables to correct axial and lateral chromatic aberrations and to control all monochromatic third-order aberrations. Significant improvements in image sizes were realized with the addition of a third lens corrector. The focal surface was almost flat, an added bonus. No penalty was incurred for a flat focal surface. Finally, each plano spectral filter was allowed to have a different thickness. In particular, because of dispersion, the aberrations and focal lengths of the lenses change with wavelength. Slight aberration differences could be introduced by changing the filter thickness and helped specifically to achieve uniform performance from band to band.

4. IMPROVED OPTICAL PERFORMANCE AND MANUFACTURABILITY

Figure 1 shows the imaging performance of the new design for each of the photometric spectral bands B, V, R, I and Z. The diameter of a focal spot that includes 80% of the polychromatic diffracted energy, as a function of radial position across the detector, is plotted. Five wavelengths, equally spanning each spectral band, were included in this analysis. For comparison, the 80% collection for a diffraction-limited telescope in the infrared Z band is also plotted (0.083 arc-seconds). The Z-band has images approximately twice the diffraction limit. Overall, the energy collection is within 0.20 arc-seconds. The energy collection of this design is quite uniform across the field for each spectral band and does not vary significantly between spectral bands. The extreme bands show the worst performance. In the near-ultraviolet B band, the lenses are very dispersive, limiting performance for a 100 nm band. In the infra-red Z band, a bandwidth of 200 nm has comparable performance.

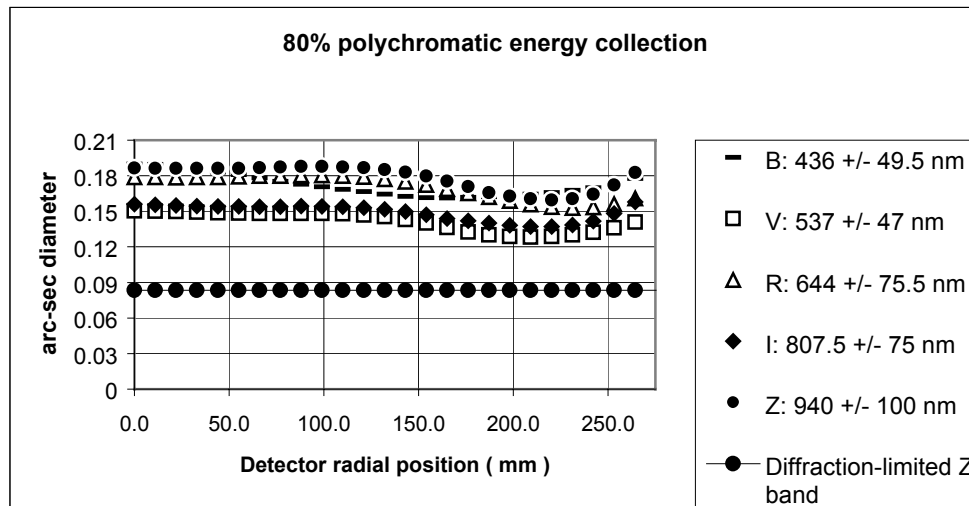


Figure 1. The image sizes that include 80% of the polychromatic diffracted energy are plotted vs. radial position on the detector for each spectral band. For comparison, the diffraction-limited 80% image for the Z-band is about 0.083 arc-sec.

The improvements were made in four main areas. First, earlier LSST designs collected 80% of the energy in one-third of arc-second images. This new design, with less than 0.20 arc-second images, represents a 40% improvement in spot size. Minimal degradation of 0.5 arc-second images will occur. Second, the most difficult optical element to fabricate and test will be the secondary mirror. The Hubble primary mirror and the LSST secondary are about the same size, 3.4 meters in diameter. However, the LSST secondary is convex. This will be the largest precision convex mirror ever manufactured by nearly a factor of two. Current testing procedures will be difficult to adapt for such a large convex mirror. To ease the burden, the aspheric departure of the secondary has been reduced to about 10 microns peak-to-valley from the best-fit sphere. Previous designs had aspheric departures 10x or higher in value. The other aspheres in this design have reduced complexity and/or reduced departures from the best-fit sphere. The primary mirror is very close to parabolic, and only departs by less than one-half of a micron from the best-fit conic. The tertiary departs only by 137 microns from the best-fit sphere. Both can be tested by an Offner-type null setup. The two largest lenses have aspheric surfaces on the concave surface, with peak-to-valley asphericities of less than 25 microns from the best-fit sphere. The smallest lens is a plano-convex spherical lens. Third, the detector surface is a flat plane, rather than a weakly curved aspheric surface required in previous designs. One can build the detector from a mosaic from many flat CCD detectors that closely match this curved surface. A flat focal plane avoids concerns about how small the detector elements must be to get a good match of the curved surface with acceptable focal errors. A flat detector can have arbitrarily sized CCD elements. The spectral filter is placed as close as possible to this last lens to minimize its size. Finally, the telescope is fully baffled so that no stray light from any field angle, involving a first reflection from the tertiary mirror, can reach the detector.

5. OPTICAL DESCRIPTION OF THE NEW TELESCOPE

The optical prescription of the telescope is given in Table 4. The first part of the table gives the design for the R band. The element radii of curvatures, vertex spacing to the next element, inner and outer diameter, and materials are given. The baffles are included as optical elements. The last column gives the aspheric departures from the best-fit sphere, fitted between the inner and outer diameters. The second part of the table gives the aspheric description of each surface, using a standard description of a conic surface plus an additional power series of even terms. The last part of the table gives the changes required to switch to a different spectral band. The amounts of displacement of the primary and tertiary mirrors along with the required spectral filter thickness are tabulated. There are several ways to compensate for focal shifts that also lead to improved focal spot size. In this particular design, three adjustments are required. First, a flat spectral filter of the appropriate band pass is inserted. The filter thickness varies between 21.5 mm at the blue end to 12.5 mm in the infrared band. Finally, both the primary and tertiary are repositioned slightly, in opposite directions. The primary moves within a range of one-third of a millimeter. The tertiary moves within a range of about 3 mm. Other possible combinations were explored, such as moving the entire detector package and moving one corrector lens. Using only two

adjustments, such as moving only the detector package and inserting a different thickness filter, resulted in about 15-20% larger focal spot sizes at the extreme spectral bands. Many other combinations of three adjustments, such as moving the detector package (detector/corrector lenses/filter) and displacing one lens element along with adjusting filter thickness, yielded similar spot sizes.

Distortion at full field is pincushion with +0.286 mm from the paraxial image location, and is mostly third order. This approximately 0.1% pincushion distortion is difficult to correct without seriously affecting the image quality. Correcting the distortion to sub-pixel throughout the field may be nearly impossible. Mapping the distortion field by using known coordinates of stars will be required in any event to accurately determine each pixel location.

The exit pupil is virtual and is located about 5.0 m past the spectral filter. The optical design of the interference band-pass filter coating could be made simpler by keeping the chief ray angle of incidence zero at all field points, that is, by curving the filters around the exit pupil. Each filter is then a meniscus element with radii of curvature of 5.0 m concave and convex. The included angle of incidence for an f/1.25 beam (NA = 0.4) is +/- 23.6 degrees. For a plane parallel spectral filter, the chief ray has a maximum angle of incidence of about 3.1 degrees. Therefore, curving the filter allows the angle of incidence over which the filter must be designed to decrease from 26.7 degrees to 23.6 degrees. Either choice gives equivalent image sizes. The final shape of the filter will involve a tradeoff between coating and optical fabrication difficulties.

No correction for atmospheric dispersion or ADC has been incorporated. The extremely fast focal ratio and the expected rapid pointing changes during the course of observations preclude any compensation technique. Reduced image quality will have to be accepted at the lower wavelength bands at angles away from the zenith.

Optical design data for R spectral band [all units mm]

Surface number	Radius of curvature	Spacing	Semi-diameter	Hole semi-diameter	Material	Description	Sag from best-fit sphere
Outer baffle		710 below secondary	4330	2185			
1	-17897.0	-5309.996	4200	2300	Reflect	primary	~parabolic
2	-6693.0	9200.0	1700	750	Reflect	secondary	10 microns
Inner baffle		630 above primary	2175	630			
3	-9466.0	-4418.0	2600	450	Reflect	tertiary	137 microns
4	-2065.0	-48.6	625	none	silica	1st aspheric lens	25 microns
5	-2902.0	-384.5	625	none			
6	-6682.0	-20.0	465	none	silica	2nd aspheric lens	25 microns
7	-1669.0	-239.0	440	none			
8	plano	-16.0	340	none	silica	dichroic filter	
9	plano	-22.0	340	none			
10	-2545.0	-30.1	320	none	silica	3rd spherical lens	
11	plano	-50.0	320	none			
Image	plano		275	none		detector	

Conic constants and polynomial aspheric data

Surface number	Conic constant	4th order	6th order	8th order	10th order
1	-0.99804	0	-2.266E-24	0	0
2	-0.1185	0	-8.578E-21	-3.063E-28	-2.275E-35
3	0.08228	0	8.575E-23	1.527E-30	0
5	0.4664	0	4.493E-18	0	0
7	-0.3177	0	-3.350E-17	0	0

Band	λ [nm]	Focal adjustments for each spectral band		
		Primary motion	Tertiary motion	Filter thickness
B	436 +/- 49.5	-0.180	1.950	21.50
V	537 +/- 47.0	-0.100	0.872	18.40
R	644 +/- 75.5	0.000	0.000	16.00
I	807.5 +/- 75	0.140	-0.980	13.40
Z	940 +/- 100	0.160	-1.280	12.50

Table 4. Optical design prescription for the R band, including aspheric terms and baffle location and sizes. The adjustments required to shift spectral bands are also included.

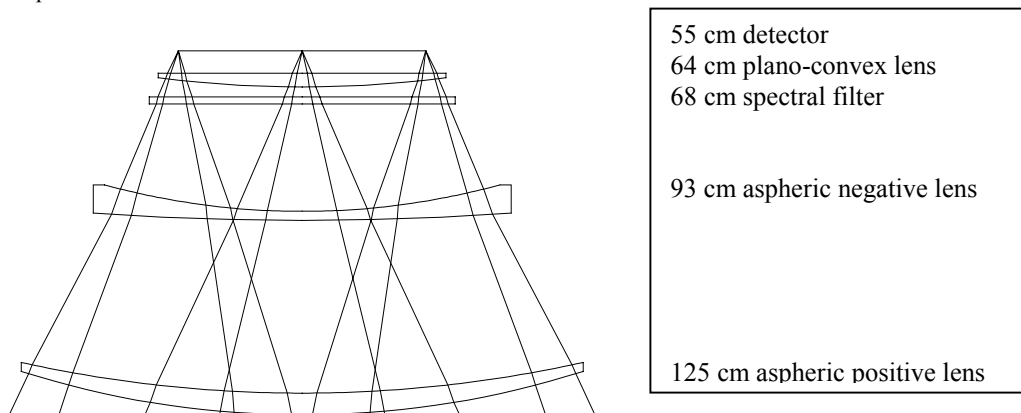


Figure 2 Flat detector, filter and triplet corrector

Optical layout drawings are given in Figure 2 and 3. Figure 2 shows the limiting rays for three points on-axis and at the full field angle. The corrector lenses range in size from 1.25 m in diameter to 0.64 m. The largest two lenses have aspheric surfaces on the concave surface, with peak-to-valley asphericities of less than 25 microns from the best-fit sphere. The smallest lens is a plano-convex spherical lens. The spectral filter was placed as close as possible to this last lens to minimize its size, and is about 0.68 m in diameter. A mechanical filter can be inserted between the first two lenses. There is room to fit the mechanism in without further obscuring the telescope. The optical performance can be improved by either decreasing the axial thickness of components or by lengthening the lens package. However, both changes lead to more difficulties in fabrication since they act to increase the diameter-to-thickness ratio.

6. BAFFLING OF THE TELESCOPE

Baffling of the telescope is required so that no light that directly reaches the tertiary mirror can be directed onto the detector. Light from angles exceeding the field of view (± 1.5 degrees) must be considered. Figure 3 shows the limiting rays for an object point on the optical axis. Straight lines just below the secondary mirror (first outer baffle with inner diameter of 4.37 m) and just above the primary mirrors (second inner baffle with outer diameter of 4.35 m) indicate the clear areas of baffles. The inner second baffle is just slightly smaller in diameter than the hole in the first outer baffle, ensuring that no light from an on-axis point can reach the tertiary. Note that some light can directly reach the tertiary, if the baffles are not in place. Incoming light that misses the primary will be reflected directly from the tertiary mirror toward the detector. However, this light is focused near the first corrector lens, sufficiently far from the detector so

that the detector hides in the hole of the beam. The detector is protected by the hole in the beam from the defocused beam. For field angles greater than 0.3 degrees, light starts to reach the tertiary with both baffles in place. However, this is not a concern. Figure 4 shows the stray light in relation to the 55 cm detector, if there were no vignetting by the lens corrector. The small amount of light in the partial annulus comfortably misses the detector. The filter and the last lens actually vignette this annulus. The two baffles ensure that, for any field angle, no directly reflected rays can reach the detector.

Previous designs were baffled to protect the detector only from light within the specified full field angle. These designs have collimated beams reflected from the secondary, with angular magnification of 2.5. Light at the full field angle of 1.5 degrees is reflected at 1.5 x 2.5 or 3.75 degrees from the secondary. Incoming light, at a field angle of 3.75 degrees, looks very much like light reflected from the secondary at full field angle. Therefore, previous designs had light reaching the detector at field angles between 1.5 and 3.75 degrees. This light, although badly aberrated and highly vignetted, is nominally in focus. The contributions of light from all objects within a field area about 6 times greater would lead to confusing background signals. Proper baffling using this criterion would have led to increased obscuration at full field.

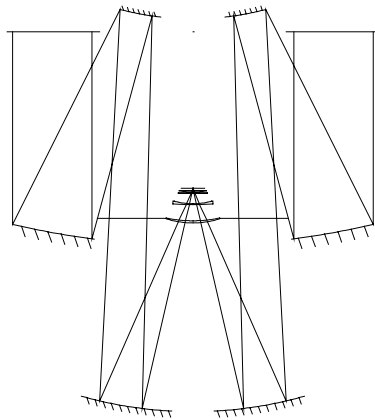


Figure 3. Optical layout of LSST: rays from an on-axis point

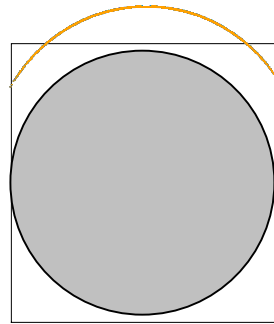


Figure 4. Stray light from 0.3 degrees in relation to the 55 cm detector

7. GHOST REFLECTIONS

Ghosts are not a significant problem. There are a total of 28 double-reflection ghosts from the 8 surfaces of the triplet lens and the filter. Many of these ghosts completely miss the detector because they are so out of focus. An analysis of all double-reflection ghosts showed that the ghost that comes closest to focusing at the detector surface involves two reflections from the spectral filter. Figure 5 shows this double-reflection ghost from each surface of the thinnest spectral filter, 12.5 mm in thickness. The ghost footprint on the detector, shown in figure 6, is a halo 14 mm in diameter, centered on the assumed 25-micron image (0.5 arc-second image). One can estimate the relative intensity of ghost image to primary image, by comparing relative areas and taking into account the reflection losses. Simple geometry gives a relationship between the ghost halo of diameter G and an image of diameter S.

$$I_{rel} = R_1 R_2 S^2 / [(1 - \epsilon^2) G^2], \quad \begin{aligned} S &= \text{image diameter} = 0.025 \text{ mm} \\ \epsilon &= \text{linear obscuration ratio} = 0.548 \\ G &= \text{ghost image diameter} = 14 \text{ mm} \\ R &= \text{surface reflectivities} = 0.01 \text{ per surface} \end{aligned}$$

$$I_{rel} = 4.6 \times 10^{-10} = \sim 23 \text{ visual magnitude difference}$$

Assuming a 1% reflection from each surface, the ghost halo is almost 10 orders of magnitude dimmer than the actual image, or a visual magnitude difference of about 23. Only ghosts from very bright objects will be visible, and these ghosts will be localized around those objects. There are approximately 1700 sky objects with a VM of 4 or less, on the

average of one object per telescope exposure. The remaining objects in the field of view will have ghosts dimmer than VM 27 or greater.

Using a curved spectral filter as described in Section 5 will not appreciable change this analysis, provided that both surfaces have the same curvature.

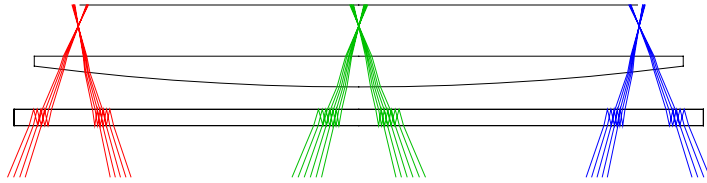


Figure 5. Double-reflection ghost from the spectral filter

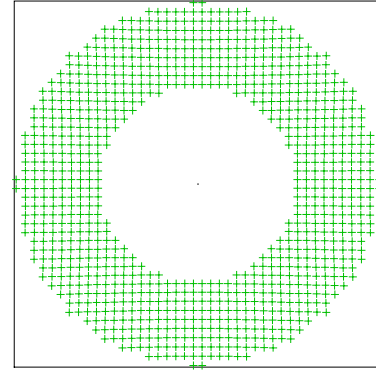


Figure 6. The double-reflection ghost from the filter is 14 mm in diameter, centered about the assumed 25-micron image

SUMMARY

In summary, an improved design for the LSST has been presented that shows a 40% reduction in focal spot size from previous designs. The convex secondary mirror and the corrector lenses have reduced asphericities that will lead to easier fabrication. The focal plane is now flat, rather than weakly curved. The detector is fully baffled against directly reflected light coming directly from the tertiary mirror. Ghosts will not be a significant problem and can be mitigated by proper design of the spectral filters.

REFERENCES

1. J. Anthony Tyson and the LSST Collaboration, "Large Synoptic Survey Telescope: Overview", Proc. SPIE 4836 (2002)
2. M. Paul, Rev d 'Optique, **14**, p. 169 (1935)
3. R. N. Wilson, *Reflecting Telescope Optics I*, pp. 215-229, A&A Library, Springer, 1996
4. J. G. Baker, IEEE Trans. Aerosp. Electron. Syst., **5**, 261 (1969)
5. R. V. Willstrop, MNRAS, **210**, p597 (1984)
6. R. Angel, M. Lesser & R. Sarlot, ASP Conference Series, Vol. 195, (2000)

***This work was performed under the auspices of the U.S. Department of Energy by Lawrence Livermore National Laboratory under Contract No. W-7405-Eng-48.**